OPTIMIZED DESIGN OF SONOTRODES FOR PIEZOELECTRIC TRANSDUCERS USING TOPOLOGY OPTIMIZATION

César Yukishigue Kiyono, ckiyono@gmail.com
Ronny Calixto Carbonari, ronny@usp.br
Emílio Carlos Nelli Silva, ecnsilva@usp.br
Department of Mechatronics and Mechanical Systems Engineering, Escola Politécnica da Universidade de São Paulo,
Av. Prof. Mello Moraes, 2231, 05508-900, São Paulo, SP, Brazil.

Abstract. *This work aims to perform the design optimization of a sonotrode, a structure usually connected to a high power piezoelectric transducer, which is a device capable of converting electric energy into mechanical displacement or vice-versa. A sonotrode transmits mechanical vibrations generated by a piezoelectric transducer, adjusting the amplitude and the distribution of these vibrations to fit the design needs for a certain application. Among applications of piezoelectric transducers using sonotrodes, we can cite navigation sonars, ultrasonic cleaning and melting devices, acoustic tomography, ultrasonic drilling machine, ultrasonic fabric cutting machine, etc. The design needs of a sonotrode differs for each application, ranging from obtaining maximum displacement in one single point of its structure, to obtaining uniform displacements on a whole face of the sonotrode. To improve the attainment of the optimum result, in this work, Topology Optimization (TO) is applied to design the sonotrode. TO is a procedure to design the optimal layout of structures by distributing material within a fixed domain. The objective of the developed TO formulation is to find the best topology of the sonotrode that produces maximum and uniform displacements at one of its face, granting that the first resonance frequency must be larger than a specified value. The TO method is implemented using the Sequential Linear Programming (SLP) as optimization algorithm, and it is based on the SIMP (Solid Isotropic Material with Penalization) and RAMP (Rational Approximation of Material Properties) interpolations for material model formulations. Finite Element Method (FEM) is applied to model the sonotrode using piezoelectric four-node axisymmetric elements. A node-based design variable implementation for continuum structural topology optimization is presented to minimize numerical instabilities such as checkerboard pattern. Resonance frequencies are computed through Lanczos method and a frequency constraint is included in the topology optimization formulation. Different optimized shapes of the sonotrode are designed, and compared with traditional designs found in the literature to verify the improvement.*

Keywords: *Sonotrode, Topology Optimization, RAMP, Piezoelectric Finite Element Method, Lanczos Eigensolver.*

1. INTRODUCTION

High power piezoelectric transducers are based on the piezoelectric effect, which is defined as the mechanical energy to electrical energy conversion (direct effect) or the electrical energy to mechanical energy conversion (inverse effect). These devices can be found in projects such as navigation sonars (Desilets et al. 1999), high power ultrasonic transducers, underwater data acoustic transmission device, ultrasonic cleaning and melting machines (Shuyu 1995, 2004, 2005, 1997), sound projector for acoustic tomography and global oceans monitoring (Morozov and Webb 2003), chemical processes (Heikkola and Laitinen 2005), fabric ultrasonic cutting and melting machines (Lucas et al. 1996), even in ultrasonic drilling device (Sherrit et al. 2000), one of NASA's recent research for Mars expeditions on other low-gravity planets.

High power piezoelectric transducers (Fig. 1(a)) are built, in general, using sandwiched shapes. The piezoelectric ceramics are pre-stressed between two metallic masses by a high-resistant mechanical screw. The two metallic masses lower the device resonance frequency well below that of the piezo stack (Desilets et al. 1999). Pre-stress prevents fracture due to high voltage applied to the ceramics (Arnold and Muhlen 2001b). Pre-stress typical value is 30 MPa (Arnold and Muhlen 2001a). Therefore, this configuration allows high electrical voltage application (kV), however, the operational frequency must be moderate (kHz).

Usually, high power piezoelectric transducers designs are connected to a sonotrode. Sonotrodes are syntonized elements used in some high power applications where they usually operate as a tool acting directly in the working surface (Lucas and Smith 1997; Cardoni and Lucas 2002), transmitting the mechanical vibration generated by the piezoelectric transducer, adjusting the amplitude and the distribution of these vibrations to satisfy the design needs.

Two types of sonotrodes are generally used in the majority of the ultrasonic applications: the cylindrical ones (Parrini 2001, 2003a, 2003b) (Fig. 1(b)) or, the blade-wide type ones (Ensminger 1988) (Fig 1(c)), depending on the displacement pattern to be produced. The cylindrical sonotrodes are applied where the region submitted to ultrasound is small, order of $50\ mm$; whereas blade-wide type sonotrodes are applied where the region submitted to the process is wider ($200\ mm$). Both cylindrical sonotrodes and the blade-wide type ones are designed to vibrate in longitudinal direction, acting as half wave length resonators. These sonotrodes usually possess a spaced out profile, which produces an amplification relation that is given by the ratio between the two tips areas of sonotrodes.

The objective of this work is to apply topology optimization techniques to design the sonotrode aiming to guarantee

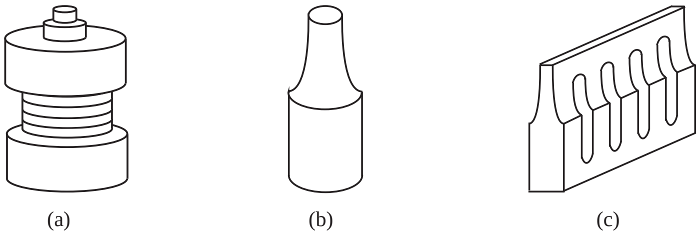

Figure 1. Schematical representation of (a) High Power Piezoelectric Transducer, (b) Cylindrical Sonotrode and (c) Blade-Wide Sonotrode.

the maximization and the uniformization of the displacements distribution in one single face of the sonotrode, helping the first resonance frequency to be larger than a specified frequency.The uniformization goal is to reduce the difference between the maximum and minimum displacements of the sonotrode face.

The application of topology optimization techniques makes the design process more efficient, with less computational cost, guaranteeing that the result is as optimized as possible.

2. PIEZOELECTRICITY

The piezoelectricity is a property that certain materials present that can be defined as the electric polarization produced by a mechanical strain in certain crystals, that is, when the piezoelectric material is submitted to a mechanical strain, an electric field is generated. The inverse effect is also applied. The constitutive equations that define the linear piezoelectric material behavior are given by (Ikeda 1996; Lerch 1990):

$$\begin{aligned}\mathbf{T} &= \mathbf{c}^E\mathbf{S} - \mathbf{e}^t\mathbf{E}\\ \mathbf{D} &= \mathbf{e}\mathbf{S} + \boldsymbol{\varepsilon}^S\mathbf{E}\end{aligned} \tag{1}$$

where $\mathbf{T}$, $\mathbf{S}$, $\mathbf{D}$ and $\mathbf{E}$ are the mechanical stress and strain, electrical charge and field tensors, respectively. $\mathbf{c}^E$, $\mathbf{e}$ and $\boldsymbol{\varepsilon}^S$ are the elastic stiffness, piezoelectric, and dielectric property matrices, respectively, which, for the $6\ mm$ symmetry class, are given by (Ikeda 1996):

$$\mathbf{c}^E = \begin{bmatrix} c_{11}^E & c_{12}^E & c_{13}^E & 0 & 0 & 0\\ c_{12}^E & c_{22}^E & c_{13}^E & 0 & 0 & 0\\ c_{13}^E & c_{13}^E & c_{33}^E & 0 & 0 & 0\\ 0 & 0 & 0 & c_{44}^E & 0 & 0\\ 0 & 0 & 0 & 0 & c_{44}^E & 0\\ 0 & 0 & 0 & 0 & 0 & c_{66}^E \end{bmatrix};\mathbf{e} = \begin{bmatrix} 0 & 0 & 0 & 0 & e_{15} & 0\\ 0 & 0 & 0 & e_{15} & 0 & 0\\ e_{31} & e_{31} & e_{33} & 0 & 0 & 0 \end{bmatrix};\boldsymbol{\varepsilon}^S = \begin{bmatrix} \varepsilon_{11}^S & 0 & 0\\ 0 & \varepsilon_{11}^S & 0\\ 0 & 0 & \varepsilon_{33}^S \end{bmatrix} \tag{2}$$

3. PIEZOELECTRIC FINITE ELEMENT METHOD

A general method such as the Finite Element Method (FEM) is necessary for the structural analysis since structure with complex topologies are expected. Therefore, the formulation of FEM for linear piezoelectricity is applied. This formulation is well-developed and only a brief description will be given here. Piezoelectric mechanisms considered for design operate in medium frequencies (kHz). Two element formulations are applied to this work, the axisymmetric and plane stress (EPTM) isoparametric four-node element formulations. Thus, using these element formulations, the global equilibrium equations are given by:

$$\left(\begin{bmatrix} \mathbf{K}_{uu} & \mathbf{K}_{u\phi}\\ \mathbf{K}_{\phi u} & \mathbf{K}_{\phi\phi} \end{bmatrix} - \omega^2 \begin{bmatrix} \mathbf{M}_{uu} & 0\\ 0 & 0 \end{bmatrix}\right)\begin{Bmatrix} \mathbf{U}\\ \mathbf{\Phi} \end{Bmatrix} = \begin{Bmatrix} \mathbf{F}\\ \mathbf{Q} \end{Bmatrix} \Longrightarrow \left[\widetilde{\mathbf{K}}\right]\{\mathbf{\Psi}\} = \{\mathbf{\Gamma}\} \tag{3}$$

where ω is the operating frequency, $\mathbf{M}_{uu}$, $\mathbf{K}_{uu}$, $\mathbf{K}_{u\phi}$, and $\mathbf{K}_{\phi\phi}$ are the mass, stiffness, piezoelectric, and dielectric matrices of the transducer, respectively. $\mathbf{U}$, $\mathbf{\Phi}$, $\mathbf{F}$ and $\mathbf{Q}$ are the mechanical displacement, electrical potential, mechanical loading, and electrical charge vectors, respectively.

It is also necessary to calculate the resonance frequencies and modes. To calculate them the electrodes are short-circuited, i.e., the degrees of freedom (DOF's) referring to the electrical potential in all electrodes must be equal to zero ($\mathbf{\Phi}_{electrodes} = 0$) in Eq. (3), and also, it must be considered $\mathbf{F} = 0$ (Guo et al. 1992; Naillon et al. 1983). Then, the resonance frequencies and modes are obtained solving the following expression:

$$\left(\left[\widehat{\mathbf{K}}\right] - \lambda\left[\widehat{\mathbf{M}}\right]\right)\{\mathbf{W}\} = 0 \quad ; \quad \lambda = \omega^2 \tag{4}$$

where λ is the eigenvalue, $\{\mathbf{W}\}$ is the eigenvector. $\left[\widehat{\mathbf{K}}\right]$ and $\left[\widehat{\mathbf{M}}\right]$ are the stiffness and mass global matrices, respectively, which include the boundary condition information for the modal analysis, that is, the FEM matrices must be obtained with the piezoelectric ceramics electrodes grounded.

4. TOPOLOGY OPTIMIZATION

Topology optimization is a powerful structural optimization technique that combines the Finite Element Method (FEM) with an optimization algorithm to find the optimal material distribution inside a given domain bounded by supports and applied loads that contains the unknown structure (Bendsøe and Sigmund 1999; Bendsøe and Kikichi 1988).

The discrete material distribution function (0–1) is an ill-posed problem (Bendsøe and Sigmund 1999), and to overcome this, the optimization problem must be relaxed by allowing the material to assume intermediate materials during the optimization. This is achieved by defining an appropriate continuous material model which defines the material transition at each point of domain.

The material model used in this work is based on the SIMP (Solid Isotropic Material with Penalization) (Bendsøe and Sigmund 1999) and the RAMP (Rational Approximation of Material Properties) (Stolpe and Svanberg 2001; Bendsøe and Sigmund 2003; Hansen 2005). The SIMP model is applied to the mass matrix, acting on the density ($\rho(\mathbf{x})$) of the structure, and the RAMP model is applied to the stiffness matrix, acting on the elasticity modulus ($E(\mathbf{x})$) of the structure. These different models are applied to reduce the localized eigenmodes in areas where the design variables assume low values (Pedersen 2000). The formulation for intermediate materials defines the level of problem relaxation (Bendsøe and Sigmund 1999).

Recent works (Matsui and Terada 2004; Rahmatalla and Swan 2004) have suggested considering the continuous distribution of the design variable inside the finite element by interpolating it using the FE shape functions. In this case, the design variables are defined for each element node, instead of each finite element as usual. This formulation, known as CAMD (Continuous Approximation of Material Distribution) seems to reduce instabilities, such as checkerboard of the material layout designs (Rahmatalla and Swan 2004).

Thus, $\rho(\mathbf{x})$ and $E(\mathbf{x})$ are given by:

$$\rho(\mathbf{x}) = \gamma(\mathbf{x})^q \rho_0 \quad ; \quad E(\mathbf{x}) = E_{min} + \frac{\gamma(\mathbf{x})}{1 + p(1 - \gamma(\mathbf{x}))}(E_0 - E_{min}) \tag{5}$$

where ρ and E are the density and the elasticity modulus properties, respectively, of the material at each point of the domain. ρ_0 and E_0 are the values of the isotropic material property. E_{min} is the minimum admissible value for the elasticity modulus. γ is the design variable, p and q are the penalizations for the stiffness and density, respectively.

5. DESIGN PROBLEM FORMULATION

The objective of this work is to define a topology optimization formulation to: uniform and maximize the displacements configuration at one given region of the sonotrode; granting that the sonotrode first resonance frequency must be either larger or equal to a specified frequency; guarantee a certain stiffness for the structure, which vibrates due to harmonic excitation of a high power piezoelectric transducer. A figure illustrating the definition of the problem of TO, as well as of the design domain and boundary conditions is presented.

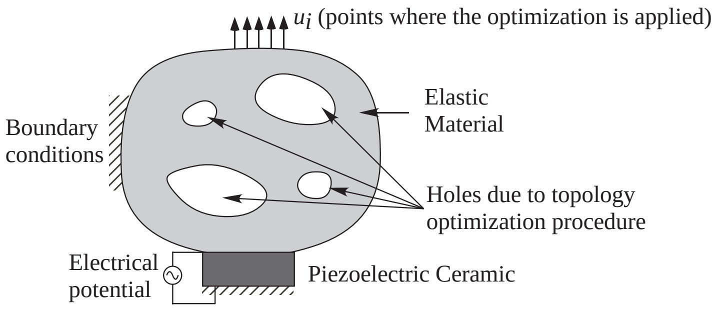

Figure 2. Definition of TO problem, design domain and boundary conditions.

The uniformization is obtained by minimizing the square summation of the difference between the displacement at each point of the region where the uniformization is desired (u_i) and a constant (β). In this kind of formulation, the objective is to approach the displacements u_i to the constant β, so that this summation becomes small through the iterations.

The maximization of displacements is obtained following the mean transduction principle (Silva 2003; Carbonari et al. 2005), which is achieved by applying the reciprocity theorem (or Betti's theorem) (Timoshenko and Goodier 1970) extended to the piezoelectric medium. This formulation gives the maximum displacement generated at specified regions and directions due to electric potential excitation in the piezoelectric medium (electric charge or potentials).

To guarantee the sonotrode stiffness, the principle of mean compliance (Silva et al. 1999; Carbonari et al. 2005) must be used. The structural function must generate enough stiffness to resist the loads during the actuation movement, as the actuator keeps its deflection at the requested regions while it is subjected to electric potentials. The mean compliance is applied assuming static behavior.

Thus, the uniformization (L_1) and the maximization (L_2) of the displacements functions and the maximization of the stiffness function (L_3) are given by the expressions:

$$L_1 = \sum_{i=1}^{m}(u_i - \beta)^2 \quad ; \quad L_2 = \int_{\Upsilon_{t_2}} \widetilde{\mathbf{t}}_2 \mathbf{u}_1 d\Upsilon \quad ; \quad L_2 = \int_{\Upsilon_{t_2}} \mathbf{t}_3 \mathbf{u}_3 d\Upsilon \tag{6}$$

where m is the number of points that are considered in the optimization procedure. $\mathbf{u}_1$ is the dynamic displacement of the sonotrode due to dynamic electric potential excitation $\widetilde{\phi}_1 = \phi_1 e^{j\omega t}$, $\widetilde{t}_2 = t_2 e^{j\omega t}$ are the unit dynamic mechanic loads, and Υ_{t_2} is the region which is submitted to optimization procedure. $\mathbf{t}_3 = -\mathbf{t}_2$ and $\mathbf{u}_3$ is the sonotrode static displacement due to load $\mathbf{t}_3$.

The three former formulations L_1, L_2, and L_3 must be combined to minimize L_1 and L_3, and maximize L_2. The following multi-objective function is proposed:

$$F = w(g \ln L_2^2 - (1-g)\ln L_1) - (1-w)\ln L_3 \tag{7}$$

where w and g are the weight coefficients that varies from 0 to 1, and allow us to control the priority of each objective function.

Thus, the topology optimization problem formulation is defined as:

$$\begin{array}{ll} \text{Maximize:} & \mathcal{F}(\gamma) \\ \quad \gamma(\mathbf{x}) & \\ \text{subject to:} & \mathbf{t}_3 = -\mathbf{t}_2 \\ & \text{Equilibrium equations} \\ & \omega_r \geq \omega_0 \\ & 0 \leq \gamma \leq 1 \\ & \int_\Omega \gamma d\Omega \leq \Theta_{lim} \end{array} \tag{8}$$

where ω_r is the resonance frequency and ω_0 is the frequency constraint value, respectively, and Θ_{lim} is the maximum volume value allowed for optimum topology.

6. NUMERICAL IMPLEMENTATION

In this work, the continuous distribution of design variable γ is given by (Matsui and Terada 2004; Rahmatalla and Swan 2004):

$$\gamma(\mathbf{x}) = \sum_{i=1}^{n_d} \gamma_i N_i(\mathbf{x}) \tag{9}$$

where γ_i is the nodal design variable, N_i is the finite element shape function and n_d is the number of nodes at each finite element. The design variable γ can assume different values at each finite element node. Due to the definition of Eq. (9), the material property functions (Eq. (5)) will also have a continuous distribution inside the design domain. Thus, considering the mathematical definitions of the stiffness and piezoelectric matrices of Eq. (3), the material properties must remain inside the integrals and be integrated together by using the graded finite element concept (Kim and Paulino 2002).

The functions L_1, L_2, and L_3 can be calculated numerically through the expressions:

$$L_1 = \{\mathbf{\Gamma}_2\}^t \left(\left\{\widetilde{\mathbf{\Psi}}_1\right\} - \{\boldsymbol{\beta}\}\right)^2 \quad ; \quad L_2 = \{\mathbf{\Gamma}_2\}^t \left\{\widetilde{\mathbf{\Psi}}_1\right\} \quad ; \quad L_3 = \{\mathbf{\Gamma}_3\}^t \{\mathbf{\Psi}_3\} \tag{10}$$

where

$$\{\mathbf{\Gamma}_2\} = \left\{ \begin{array}{c} \mathbf{F}_2 \\ 0 \end{array} \right\} = -\{\mathbf{\Gamma}_3\} \;\; ; \;\; \left\{\widetilde{\mathbf{\Psi}}_\mathbf{1}\right\} = \left[\widetilde{\mathbf{K}}\right]^{-1} \left\{\widetilde{\mathbf{\Gamma}}_\mathbf{1}\right\} \;\; ; \;\; \{\mathbf{\Psi_3}\} = [\mathbf{K}]^{-1}\{\mathbf{\Gamma_3}\} \;\; ; \;\; \{\boldsymbol{\beta}\} = \left\{ \begin{array}{c} \beta \\ \beta \\ \beta \\ \vdots \\ \beta \\ \beta \end{array} \right\} \tag{11}$$

with $\mathbf{F}_2$ as the mechanical load vector $\mathbf{t}_2$ and $\left\{\widetilde{\mathbf{\Gamma}}_\mathbf{1}\right\}$ as the electric potential vector ϕ_1. $[\mathbf{K}]$ is the static stiffness matrix of the structure and $\left[\widetilde{\mathbf{K}}\right]$ is the dynamic matrix of the problem, involving the stiffness and mass matrices, modified for electrical potential excitation. Vector $\{\boldsymbol{\beta}\}$ has the same length of the vector $\left\{\widetilde{\mathbf{\Psi}}_\mathbf{1}\right\}$.

Thus, the discretized form of the final optimization problem is stated as:

$$
\begin{array}{ll}
\underset{\gamma}{\text{Maximize:}} & \mathcal{F}(\gamma) \\
\text{subject to:} & \{\mathbf{\Gamma}_3\} = -\{\mathbf{\Gamma}_2\} \\
& \left[\widetilde{\mathbf{K}}\right]\left\{\widetilde{\mathbf{\Psi}}_1\right\} = \left\{\widetilde{\mathbf{\Gamma}}_1\right\} \\
& \left[\widetilde{\mathbf{K}}\right]\left\{\widetilde{\mathbf{\Psi}}_2\right\} = \left\{\widetilde{\mathbf{\Gamma}}_2\right\} \\
& [\mathbf{K}]\{\mathbf{\Psi}_3\} = \{\mathbf{\Gamma}_3\} \\
& \left(\left[\widehat{\mathbf{K}}\right] - \lambda\left[\widehat{\mathbf{M}}\right]\right)\{\mathbf{W}\} = 0 \\
& \omega_r \geq \omega_0 \\
& 0 < \gamma_{min} \leq \gamma_i \leq 1 \qquad i = 1, \ldots, N_e \\
& \sum_{i=1}^{N_e} \gamma_i V_i^0 \leq \Theta_{lim}
\end{array}
\tag{12}
$$

where V_i^0 is the volume associated with each finite element node and is equal to finite element volume. N_e is the number of nodes in the design domain, and γ_{min} is the design variable minimum value that can be set to avoid numerical instabilities.

The mathematical programming method called Sequential Linear Programming (SLP) is applied to solve the optimization problem since there are a large number of design variables, and different objective functions and some constraints are considered (Vanderplatz 1984). The linearization of the problem (Taylor series) at each iteration requires the sensitivities (gradients) of the multi-objective function and constraints. These sensitivities will depend on gradients of L_1, L_2, and L_3 functions in relation to γ. Suitable moving limits are introduced to assure that the design variables do not change by more than $5 - 15\%$ between consecutive iterations. A new set of design variables are obtained after each iteration, and the optimization continues until convergence is achieved for the objective function. The initial values of design variables are random values. The results are obtained using the continuation method where the coefficient penalization p varies from 1 to 4 and the value of penalization coefficient q varies form 1 to 3. The continuation method minimizes the problem of the multiple local minimum (or maximum) (Stolpe and Svanberg 2001). A flow chart of the optimization algorithm describing the steps involved is shown in Fig. 3. The software was implemented using the C language.

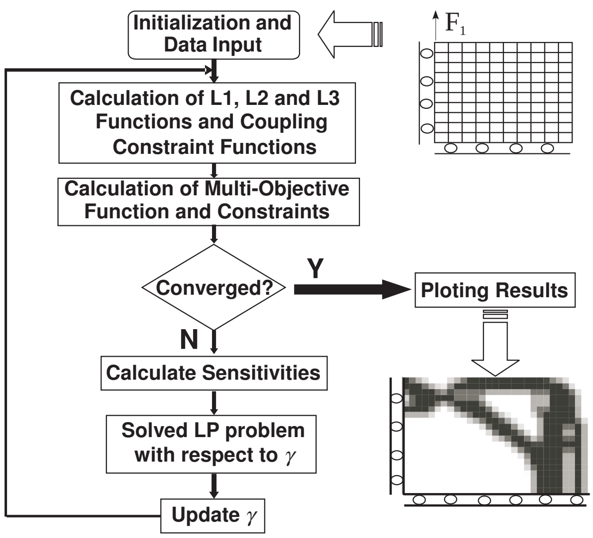

Figure 3. Flow chart of optimization procedure.

7. NUMERICAL RESULTS

Examples are presented to illustrate the design of the sonotrode using the proposed method. The idea is to simultaneously distribute non-piezoelectric and void material on regions with predefined materials, specified in the design domain, presented in Fig. 4. Table 1 presents the piezoelectric material properties used in the simulations for all examples. $\mathbf{c}^E$, $\mathbf{e}$, and $\boldsymbol{\varepsilon}^S$ are the elastic, piezoelectric and dielectric properties, respectively, of the PZT medium and ρ is the density of the

PZT material. Table 1 also presents the elasticity modulus (Young's modulus E_0), density (ρ) and Poisson's ratio (ν) of Steel 4340.

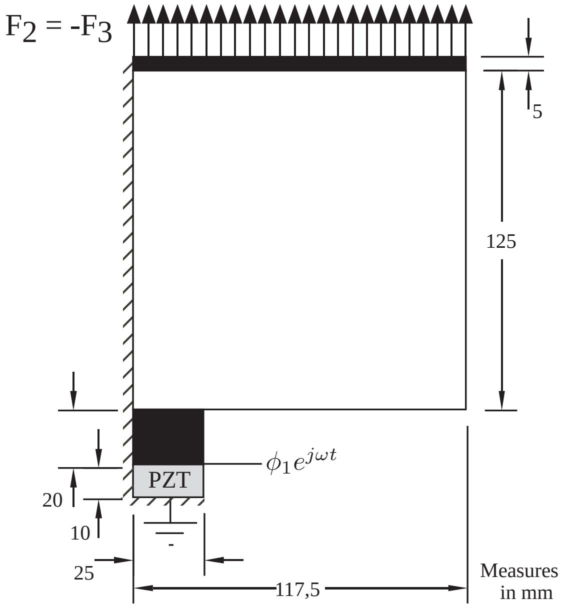

Figure 4. Design domain including loadings, constraints and measurements.

Table 1. Properties of PZT8 material and Steel 4340.

PZT8				***Steel4340***	
$c^E_{11}(10^{10}N/m^2)$	13.7	$e_{31}(C/m^2)$	-4.0		
$c^E_{12}(10^{10}N/m^2)$	6.97	$e_{33}(C/m^2)$	13.8	$E_0(GPa)$	208.3
$c^E_{13}(10^{10}N/m^2)$	7.16	$e_{15}(C/m^2)$	10.4	$\rho(kg/m^3)$	7846.3
$c^E_{33}(10^{10}N/m^2)$	12.4	$\varepsilon_{11}(10^{-9}F/m)$	7.9473	ν	0.29
$c^E_{44}(10^{10}N/m^2)$	3.4	$\varepsilon_{33}(10^{-9}F/m)$	5.1507		
$c^E_{66}(10^{10}N/m^2)$	3.365	$\rho(kg/m^3)$	7700		

The electric potential applied to piezoceramics electrodes (ϕ_1) is equal to $2000\ V$ and the operating frequency (ω) is equal to $3000\ Hz$. The optimization parameters that can be modified are the multi-objective function weights (coefficients w and g), the value of β, volume constraint (Θ_{lim}), the initial value of the design variable (γ_0), and the frequency constraint value.

β can be modified only if the design domain is changed. In this work, β is equal to 0.00001, the frequency constraint value (ω_0) chosen is equal to 2000 Hz, and $\gamma_0 = 0.25$. All examples are simulated for 50 iterations and the checkerboard filter is applied until iteration 45. The continuation method changes the value of the penalization coefficient p at iterations 15, 25 and 32, and the penalization coefficient q at iterations 25 and 32. The frequency constraint acts from iteration 45 until the end of the optimization.

The results are shown in Fig. 5 and Fig. 6 . For both results, figure (a) shows the optimal topology obtained, figure (b) shows the interpretation of the optimal topology with the boundary conditions, and figure (c) shows the deformed shape for harmonic analysis at operation frequency ($3000\ Hz$). The first result, shown in Fig. 5, topology optimization was obtained using $w = 0.40$, $g = 0.15$ and $\Theta_{lim} = 0.30$. In the second result (Figure 6), topology optimization was solved using $w = 0.45$, $g = 0.15$ and $\Theta_{lim} = 0.28$.

It is shown in Fig. 7 the deformed shape of a traditional Blade-Wide sonotrode (Fig. 1(c)) used for ultrasonic fabric cutting (Lucas et al. 1996; da Silva 2006). It is shown only the right-half of the sonotrode (symmetry conditions) and the piezoelectric excitation is at the left-bottom corner of the sonotrode (like example shown in Fig. 4).

A detailed analysis (Fig. 8) of the sonotrode desired points (u_i in Fig. 2) shows the maximum amplitude (D) of the sonotrode face, and the difference between maximum and minimum displacements (Δ). In the first result (Fig. 8(a)), $D = 0.35946\ \mu m$ and $\Delta = 9.86\%$. The second result (Fig. 8(b)) gives $D = 0.37942\ \mu m$ and $\Delta = 7.39\%$. The displacements analysis of the blade-wide sonotrode of Fig. 7 shows that $D = 0.12075\ \mu m$ and $\Delta = 10.70\%$(Fig. 8(c)).

Modal analysis of the interpreted optimum structures shows that the frequency constraint is respected for both results, $2014\ Hz$ for the first resonance frequency and $2050\ Hz$ in the second result.

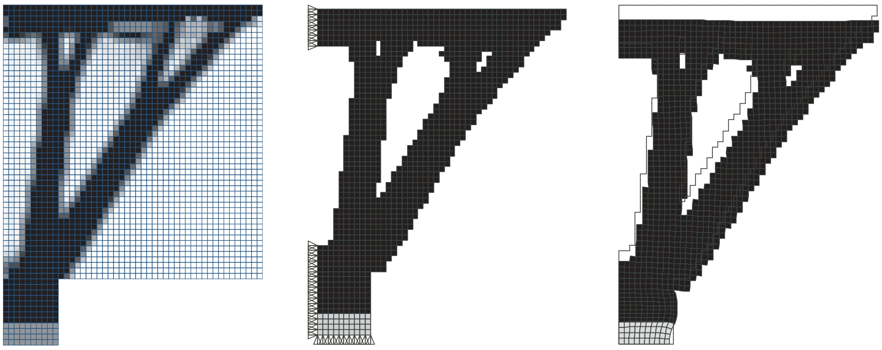

(a) (b) (c)

Figure 5. (a) Optimal topology, (b) interpretation and (c) deformed shape for $w = 0.40$, $g = 0.15$ and $\Theta_{lim} = 0.30$.

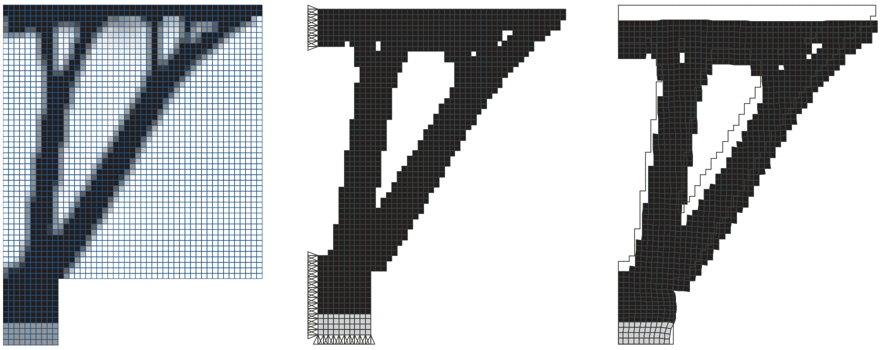

(a) (b) (c)

Figure 6. (a) Optimal topology, (b) interpretation and (c) deformed shape for $w = 0.45$, $g = 0.15$ and $\Theta_{lim} = 0.28$.

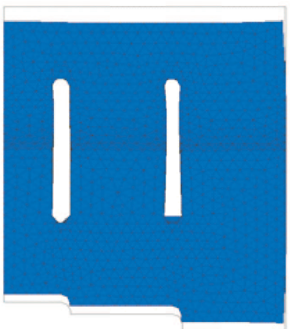

Figure 7. Deformed shape of a Blade-Wide Sonotrode used for ultrasonic fabric cutting.

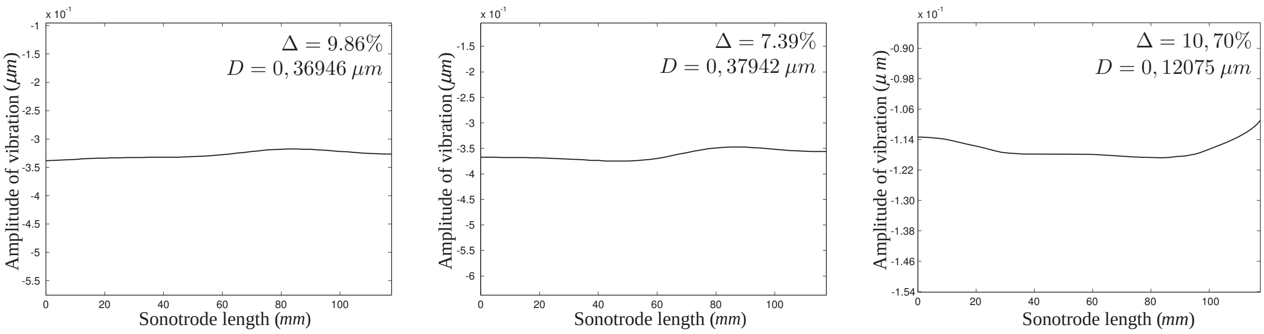

(a) (b) (c)

Figure 8. Detailed analysis of the displacement of the desired points of the sonotrode for: (a) first result ($D = 0.36946\ \mu m$ and $\Delta = 9.86\%$), (b) second result ($D = 0.37942\ \mu m$ and $\Delta = 7.39\%$), and (c) traditional blade-wide sonotrode ($D = 0.12075\ \mu m$ and $\Delta = 10.70\%$).

8. CONCLUSIONS

A topology optimization formulation was proposed which allows the simultaneous search for an optimal topology of a structure that minimizes the difference between the maximum and minimum displacements of the desired points, maximizes the displacements of these points, minimizes the flexibility of the structure, and grants that the first resonance frequency is larger than a specified value. This is achieved by the optimization problem by allowing the simultaneous distribution of non-piezoelectric and void material in the design domain and applying an electric potential as electrical excitation.

The adopted material model in the formulation is based on the density method and it interpolates fictitious densities at each finite element based on pseudo-densities defined as design variables for each finite element node providing a continuous material distribution in the domain. Some 2D examples were presented to illustrate the potentiality of the method. The examples show that the objectives were achieved, and lower differences between maximum and minimum displacements are obtained by changing the value of w, g, and the volume constraint (Θ_{lim}). Harmonic analysis of the optimum structures obtained in this work proves that these structures have more uniform displacements configuration at harmonic excitation than the traditional one, keeping the same maximum displacement value.

9. ACKNOWLEDGEMENTS

The first author thanks Fundação de Amparo à Pesquisa do Estado de São Paulo (FAPESP - Research Support Foundation of São Paulo State) for supporting him through a master fellowship (n^{o}. 05/57810-8). The second author thanks CNPq (Conselho Nacional de Desenvolvimento Científico e Tecnológico - Brazil), for supporting him through a doctoral fellowship (n^{o}. 140687/2003-3). The last author thanks FAPESP (project n^{o}. 06/57805- 7) and CNPq.

10. REFERENCES

Arnold, F. J. and S. S. Muhlen (2001a, January). The mechanical pre-stressing in ultrasonic piezotransducers. *Ultrasonics 39*(1), 7–11.

Arnold, F. J. and S. S. Muhlen (2001b, January). The resonance frequencies on mechanically pre-stressed ultrasonic piezotransducers. *Ultrasonics 39*(1), 1–5.

Bendsøe, M. P. and N. Kikichi (1988, November). Generating optimal topologies in structural design using a homogenization method. *Computer Methods In Applied Mechanics And Engineering 71*(2), 197–224.

Bendsøe, M. P. and O. Sigmund (1999, November). Material interpolation schemes in topology optimization. *Archive Of Applied Mechanics 69*(9-10), 635–654.

Bendsøe, M. P. and O. Sigmund (2003). *Topology Optimization - Theory, Methods and Applications*. New York, USA.

Carbonari, R. C., E. C. N. Silva, and S. Nishiwaki (2005, December). Design of piezoelectric multi-actuated microtools using topology optimization. *Smart Materials & Structures 14*(6), 1431–1447.

Cardoni, A. and M. Lucas (2002, May). Enhanced vibration performance of ultrasonic block horns. *Ultrasonics 40*(1-8), 365–369.

da Silva, J. B. (2006). Análise numérica de um transdutor piezelétrico de potência para processamento de termoplásticos têxteis. Master's thesis, Escola Politécnica da USP, São Paulo - Brasil.

Desilets, C., G. Wojcik, L. Nikodym, and K. Mesterton (1999). Analyses and measurements of acoustically matched, air-coupled tonpilz transducers. *IEEE Ultrasonics Symposium 1*, 1045–1048.

Ensminger, D. (1988). *Ultrasonics: Fundamentals, Technology, Applications* (2 ed.). New York, USA.

Guo, N., P. Cawley, and D. Hitchings (1992, November). The finite-element analysis of the vibration characteristics of piezoelectric disks. *Journal Of Sound And Vibration 159*(1), 115–138.

Hansen, L. V. (2005, May). Topology optimization of free vibrations of fiber laser packages. *Structural And Multidisciplinary Optimization 29*(5), 341–348.

Heikkola, E. and M. Laitinen (2005, January). Model-based optimization of ultrasonic transducers. *Ultrasonics Sonochemistry 12*(1-2), 53–57.

Ikeda, T. (1996). *Fundamentals of Piezoelectricity*. Oxford - England.

Kim, J. H. and G. H. Paulino (2002, July). Isoparametric graded finite elements for nonhomogeneous isotropic and orthotropic materials. *Journal Of Applied Mechanics-Transactions Of The Asme 69*(4), 502–514.

Lerch, R. (1990, May). Simulation of piezoelectric devices by 2-dimensional and 3-dimensional finite-elements. *Ieee Transactions On Ultrasonics Ferroelectrics And Frequency Control 37*(3), 233–247.

Lucas, M., G. Graham, and A. C. Smith (1996, June). Enhanced vibration control of an ultrasonic cutting process. *Ultrasonics 34*(2-5), 205–211.

Lucas, M. and A. C. Smith (1997, July). Redesign of ultrasonic block horns for improved vibration performance. *Journal Of Vibration And Acoustics-Transactions Of The Asme 119*(3), 410–414.

Matsui, K. and K. Terada (2004, April). Continuous approximation of material distribution for topology optimization. *International Journal For Numerical Methods In Engineering 59*(14), 1925–1944.

Morozov, A. K. and D. C. Webb (2003, April). A sound projector for acoustic tomography and global ocean monitoring. *Ieee Journal Of Oceanic Engineering 28*(2), 174–185.

Naillon, M., R. H. Coursant, and F. Besnier (1983). Analysis of piezoelectric structures by a finite-element method. *Acta Electronica 25*(4), 341–362.

Parrini, L. (2001, November). Design of advanced ultrasonic transducers for welding devices. *Ieee Transactions On Ultrasonics Ferroelectrics And Frequency Control 48*(6), 1632–1639.

Parrini, L. (2003a, January). New techniques for the design of advanced ultrasonic transducers for wire bonding. *Ieee Transactions On Electronics Packaging Manufacturing 26*(1), 37–45.

Parrini, L. (2003b, June). New technology for the design of advanced ultrasonic transducers for high-power applications. *Ultrasonics 41*(4), 261–269.

Pedersen, N. L. (2000, August). Maximization of eigenvalues using topology optimization. *Structural And Multidisciplinary Optimization 20*(1), 2–11.

Rahmatalla, S. F. and C. C. Swan (2004, May). A q4/q4 continuum structural topology optimization implementation. *Structural And Multidisciplinary Optimization 27*(1-2), 130–135.

Sherrit, S., X. Bao, Z. Chang, B. P. Dolgin, Y. Bar-Cohen, D. Pal, J. Kroh, and T. Peterson (2000). Modeling of the ultrasonic/sonic driller/corer: Usdc. *IEEE Ultrasonic Symposium 1*, 4.

Shuyu, L. (1995). Design of piezoelectric sandwich ultrasonic trasnducers with large cross-section. *Applied Acoustics 44*, 249–257.

Shuyu, L. (1997). Sandwiched piezoelectric ultrasonic transducers of longitudinal-torsional compound vibrational modes. *IEE Transactions on Ultrasonics, Ferroelectrics, and Frequency Control 44*(6), 1189–1197.

Shuyu, L. (2004). Optimization of the performance of the sandwich piezoelectric ultrasonic transducer. *Journal of Acoustical Society of America 115*(1), 182–186.

Shuyu, L. (2005). Analysis of the sandwich piezoelectric ultrasonic transducer in coupled vibration. *Journal of Acoustical Society of America 117*(2), 653–661.

Silva, E. C. N. (2003, April). Topology optimization applied to the design of linear piezoelectric motors. *Journal Of Intelligent Material Systems And Structures 14*(4-5), 309–322.

Silva, E. C. N., S. Nishiwaki, and N. Kikuchi (1999). Design of piezocomposite materials and piezoelectric transducers using topology optimization - part ii. *Archives Of Computational Methods In Engineering 6*(3), 191–222.

Stolpe, M. and K. Svanberg (2001, September). An alternative interpolation scheme for minimum compliance topology optimization. *Structural And Multidisciplinary Optimization 22*(2), 116–124.

Timoshenko, S. and J. N. Goodier (1970). *Theory of Elasticity* (3 ed.), Volume 1.

Vanderplatz, G. (1984). *Numerical Optimization Techniques for Engineering Design with Applications*. New York - USA.

11. Responsibility notice

The author(s) is (are) the only responsible for the printed material included in this paper